Homoaromaticity in Aza- and Phosphasemibullvalenes. A Computational Study.

Daniel Rodriguez Greve

Journal of Physical Organic Chemistry

Homoaromaticity in Aza- and Phosphasemibullvalenes. A Computational Study.

Journal:	*Journal of Physical Organic Chemistry*
Manuscript ID:	POC-10-0020.R1
Wiley - Manuscript type:	Research Article
Date Submitted by the Author:	02-Apr-2010
Complete List of Authors:	Greve, Daniel
Keywords:	Homoaromaticity, Semibullvalene, Azasemibullvalene, Phosphasemibullvalene

Daniel R. Greve
" Homoaromaticity in Aza- and Phosphasemibullvalenes. A Computational Study."

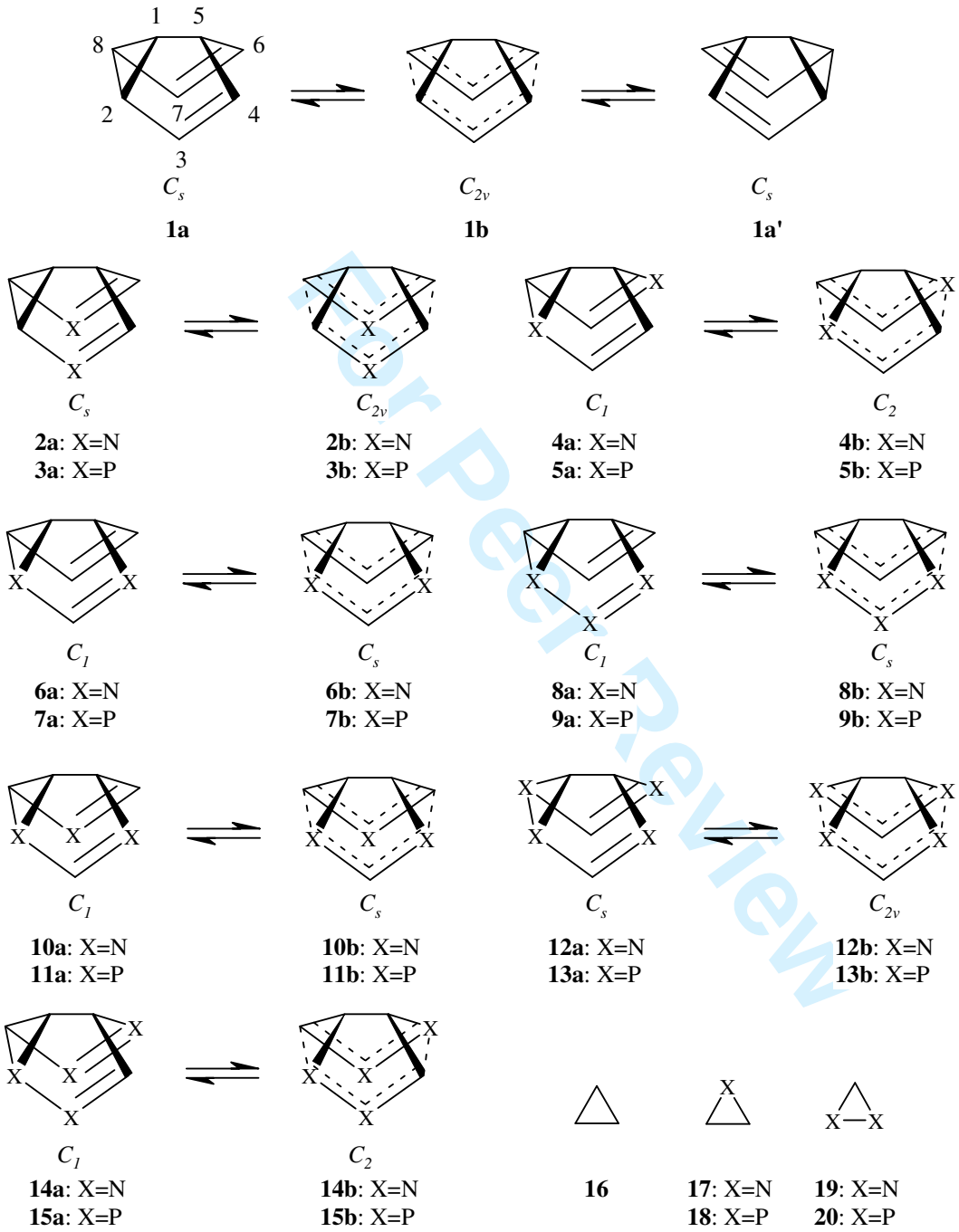

Scheme 1

Daniel R. Greve
" Homoaromaticity in Aza- and Phosphasemibullvalenes. A Computational Study."

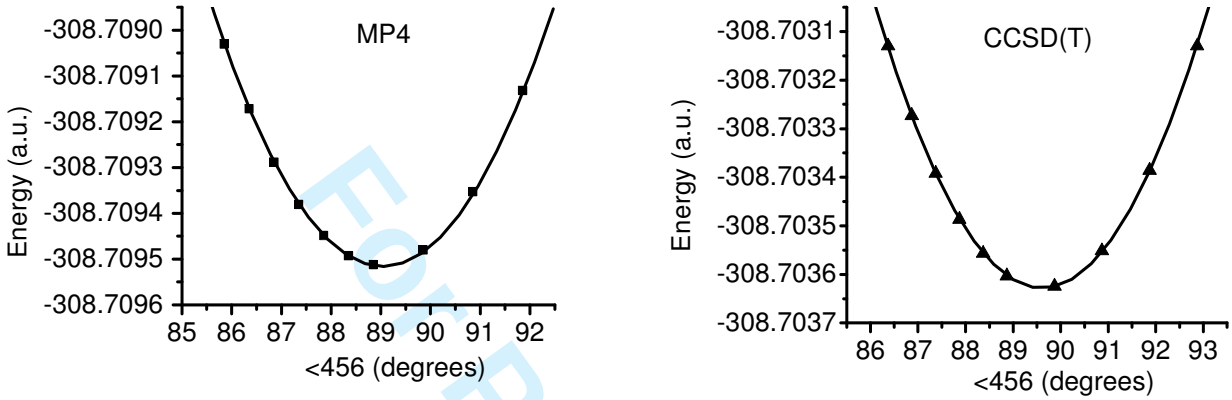

Figure 1. Calculated MP4 (left, ■) and CCSD(T) (right, ▲) energies for several *C2v* symmetric MP2 optimized **1b** geometries with fixed values of <456.Full lines are fitted quadratic potentials.

Daniel R. Greve
" Homoaromaticity in Aza- and Phosphasemibullvalenes. A Computational Study."

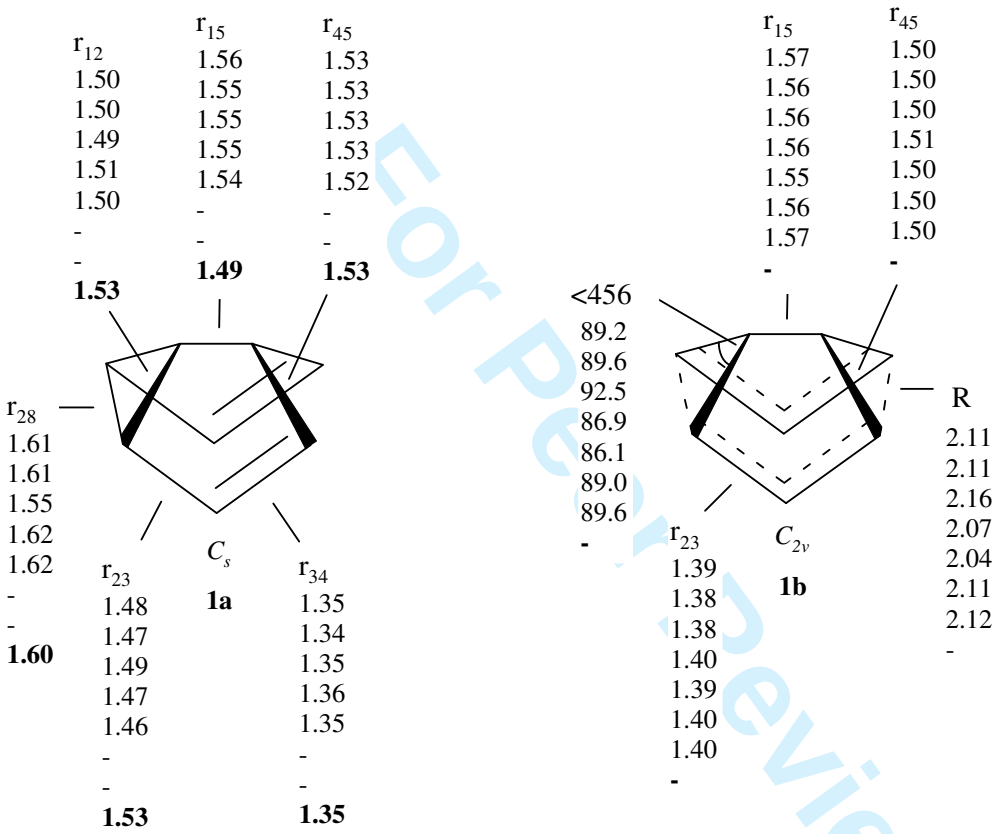

Figure 2. Calculated geometric parameters at the B3LYP, B3LYP/cc-pVTZ, (6,6)CASSCF, MP2, MP2/cc-PVTZ, MP4 (optimized <456), CCSD(T) (optimized <456) levels of theory and experimental values[46] in bold.

Homoaromaticity in Aza- and Phosphasemibullvalenes. A Computational Study.

Daniel R. Greve, Kornvænget 20, 3660 Stenløse, Denmark.
E-mail: daniel@greve-solvang.dk Phone: +45 25130229

Abstract

The ethalpies of activation $\Delta H^{\ddagger}$ for the Cope rearrangement in several aza- and phosphasemibullvalenes have been investigated by MP4/cc-pVDZ//MP2/cc-pVDZ and CCSD(T)/cc-pVDZ//MP2/cc-pVDZ calculations. One tetraazasemibullvalene and several phosphasemibullvalenes were found to have vanishing $\Delta H^{\ddagger}$ values, which together with calculated large negative Nucleus Independent Chemical Shift (NICS) values and geometrical data shows that these molecules have delocalised and bishomoaromatic minima. Furthermore, three azasemibullvalenes were found to have small $\Delta H^{\ddagger}$ values (≤2 kcal/mol) combined with large negative NICS, suggesting that they could also have bishomoaromatic minima.

Introduction

Semibullvalene (**1**) undergoes a rapid, degenerate Cope rearrangement, where the experimental enthalpy difference $\Delta H^{\ddagger}$ between the localized C_s symmetric structure **1a** and the delocalized bishomoaromatic C_{2v} symmetric transition state structure **1b** is 4.8–5.2 kcal/mol. [1,2] Over the last decades researchers have discovered and explored a wealth of structures based on **1**,[3,4] the intriguing fundamental goal being the experimental identification of a semibullvalene having a delocalized bishomoaromatic ground state. Strategies towards this goal have mainly been twofold: a) introduction of substituents[5-15] or coordinating entities[16,17] aiming at electronic stabilization of **1b** relative to **1a** and b) annelation of small rings[7,18-24] which by strain destabilizes **1a** relative to **1b**. Both strategies have been pursued by experimental and computational means, the latter proving to be a valuable tool in the search for homoaromatic structures.[5-8,11-17,19-21,23] From strategy a) Dewar et al. furthermore proposed[5,8,25] that introduction of hetero atoms in the semibullvalene skeleton could lead to a delocalized ground state. Based on semiempirical MINDO/2 and AM1 calculations, they estimated that both diazasemibullvalenes **2** and **4** would have a 'nonclassical' delocalized bishomoaromatic ground state, while tetraazasemibullvalene **12** should have a classical localized structure. Experimentally, derivatives of 2,6-diazasemibullvalene (**4**) are known.[26-28] The 1,5-dimethyl-3,7-diphenyl derivative of **4** was shown to have a lower barrier of the Cope rearrangement as compared to **1**, although still retaining a localized ground state.[26] Upon heating to 90 °C this compound rearranges to the 1,5-diazocine.[27] Attempted synthesis of derivatives of tetraazasemibullvalene **12** failed, giving 1,3,5,7-tetrazocines instead.[29] Derivatives of diphosphasemibullvalene[30] and tetraphosphasemibullvalene[31,32] have been synthesized, but none of them were observed to undergo a Cope rearrangement. However, these phosphasemibullvalenes had a P atom in the bridge, i.e. at position 1 or 5 (Scheme 1). Heteroatoms are unfavorable in these positions, since the weaker N-N and P-P bonds could result in easier breakdown of the semibullvalene skeleton, favouring valence tautomeric structures, i.e. the delocalized structure of 1,5-diazasemibullvalene was shown to be the valence tautomeric diazapentalene.[7]
Analogously to **1**, introduction of heteroatoms in the related fluxional molecule barbaralane has been investigated. Experimentally, 2,4,6,8-tetraazasubstitution slightly reduces the barrier of the Cope rearrangement,[33] and two heterobarbaralenes were shown to have homoaromatic ground states using *ab initio* computational methods.[34,35]

Hence, on basis of experimental findings and early semiempirical computational studies, a systematic study of how introduction of two or more hetero atoms in the semibullvalene skeleton affects the height of the barrier to the Cope rearrangement could lead to identification of a hetero semibullvalene based bishomoaromatic ground state structure. In this paper, the results of such a study using correlated *ab initio* computational methods are presented. The hetero semibullvalenes investigated here, **2 - 15** (Scheme 1), are generated by replacing two, three and four carbon atoms with nitrogen or phosphorus in the semibullvalene skeleton. How these replacements affects the height of the barrier to the Cope rearrangement is addressed by calculation of $\Delta H^{\ddagger}$, while the aromatic character of **2 - 15** is discussed in terms of their calculated Nucleus Independent Chemical Shift (NICS)[36] as well as calculated geometric characteristics like interallylic distances R and selected bond lengths.

Computational Methodology

All molecular geometries were optimized at the MP2 level of theory using analytical gradients, imposing the symmetries shown in Scheme 1. Using these geometries, energies where evaluated at the CCSD(T) and MP4(SDTQ) levels of theory. Vibrational frequencies and harmonic zero-point energies (ZPE) were calculated at the MP2 level of theory and are unscaled. All calculations were performed with the cc-pVDZ[37] basis set and all correlated calculations were performed with the frozen core approximation. Additionally, for **1a** and **1b** the cc-pVTZ[37] basis set was used, as were the Becke3LYP, MP3, MP4, CASSCF and CCSD computational methods. Calculations were performed using GAMESS (US) QC package[38], either as PC GAMESS[39] or as WinGamess.[40] The cc-pVDZ and cc-pVTZ basis sets were obtained from the Extensible Computational Chemistry Environment Basis Set Database.[41] Calculation of shielding tensors for determination of NICS were done at the GIAO-HF/cc-pVDZ level of theory on MP2 optimized geometries using NWChem 4.5.[42]

Results and discussion

In order to select an appropriate combination of basis set and computational level of theory, which would give calculated data of **2 - 15** with reasonable predictive value, the well-described native semibullvalene **1** was first investigated using different methods and basis sets.

Semibullvalene

The calculated values of $\Delta H^{\ddagger}$ for **1** at different levels of theory are presented in Table 1. Like all applied methods, the HF and (6,6)CASSCF methods correctly predict **1** to have a localized **1a** ground state, but they far from reproduce the experimental $\Delta H^{\ddagger}$ (compare entries 1 and 13 with 17), in agreement with earlier findings.[23] From Becke3LYP density functional theory a barrier lower than experiment is found with the cc-pVDZ basis (entry 11), which is lowered still further using cc-pVTZ (entry 12). Jiao et al.[23] (using Becke3LYP/6-31G*) and Wu et al.[15] (using Becke3LYP/6-311+G(d,p)) made similar observations. The MP2 and MP3 methods (entries 2, 3, 7 and 8) similarly give values of $\Delta H^{\ddagger}$ far from experimental result, while the calculated MP4 values (entries 4 and 9) are starting to get close. However, oscillating values of $\Delta H^{\ddagger}$ are observed in the HF, MP2, MP3 and MP4 series of calculations, using both cc-pVDZ (entries 1-4) and cc-pVTZ (entries 7-9): HF overestimates, MP2 underestimates, MP3 overestimates (but less than HF) while MP4 again underestimates $\Delta H^{\ddagger}$, but much less than MP2. Actually, the MP4 results are close to experiment (compare entries 4 and 9 with 17), although the MP4/cc-pVTZ energy at first glance appears too low. The MP results clearly converge to a limiting "MP-∞" value of $\Delta H^{\ddagger}$, which is estimated to 4.9 kcal/mol for cc-pVDZ (from entries 1-4) and 4.7 kcal/mol for cc-pVTZ (from entries 7-9), both in good agreement with the experimental value of 4.8–5.2

kcal/mol.[1,2] Such oscillating behaviour of MP calculations are well known, and often the correct answer is to be found somewhere between the MP3 and MP4 results.[43] For **1**, this is indeed true. When comparing experimental and calculated values, it should be noted that the values presented here are calculated in vacuum, while experimental $\Delta H^{\ddagger}$ were measured in CF_2Cl_2/CD_2Cl_2,[1] and furthermore, that significant solvent effects have been reported [44,45] for substituted derivatives of **1**.

The coupled cluster methods CCSD and CCSD(T) were applied using the cc-pVDZ basis. By including non-iterative triples 3.3 kcal/mol is gained in $\Delta H^{\ddagger}$ (compare entries 14 and 15) relative to the CCSD result. The CCSD(T) value is around 2 kcal/mol higher than experiment. This is in accordance with Wu et al.[15] using the 6-311+G(d,p) basis.

In an attempt to include MP4 and CCSD(T) correlation effects in the interallylic interaction, and because it was not possible to fully optimize **1b** at these levels of theory, a fitting approach was employed: Single-point MP4/cc-pVDZ and CCSD(T)/cc-pVDZ energies were calculated at several C_{2v} symmetric **1b** geometries. These geometries were optimized at the MP2/cc-pVDZ level with fixed values of the <456 angle (Figure 2 right) which controls the interallylic distance R. Fitting of the MP4 and CCSD(T) energies to quadratic potentials gave optimized <456 angles of **1b** at the MP4 and CCSD(T) levels (Figure 1). The optimal <456 angle extrapolated at the MP4 level is 89.0 degrees and at the CCSD(T) level it is 89.6 degrees (Figure 1). Hence, by including higher order correlation effects in the interallylic interaction, the two allylic subunits are moved away from each other, compared to the MP2/cc-pVDZ result of 86.9 degrees. The calculated $\Delta H^{\ddagger}$ at these angle optimized geometries are 4.91 kcal/mol for MP4 and 7.10 kcal/mol for CCSD(T) (Table 1 entries 5 and 16, Hence, around 0.2 kcal/mol are gained for both MP4 (compare entries 5 and 6) and CCSD(T) (compare entries 15 and 16) by including these correlation levels in the optimization of the interallylic interaction. The MP4 result is similar to the earlier estimated "MP-∞" value.

From the above discussion, the fact that the MP4/cc-pVDZ//MP2/cc-pVDZ value of $\Delta H^{\ddagger}$ (entry 4) agrees well with experimental values (entry 17), is not coincidental. It is clearly supported by the extrapolated "MP-∞" values (cc-pVDZ and cc-pVTZ). Hence, the MP4/cc-pVDZ//MP2/cc-pVDZ method serves as the compromise of choice with good predictive value of $\Delta H^{\ddagger}$. Additionally, the CCSD(T)/cc-pVDZ//MP2/cc-pVDZ method was applied, since this method is increasingly gaining popularity and often is referred to as an effective way of including electron correlation.

The geometry of **1a** and **1b** optimized at various levels of theory are presented in Figure 2 and compared with available experimental values.[46] As judged by Jiao,[23] the experimental[46] bond lengths r_{15} and r_{23} (Figure 2 left) in **1a** should be interchanged. Very good agreement across the different applied computational methods is observed for **1a** and the calculated bond lengths furthermore compare well with experimental values (Figure 2 left). The r_{23} and r_{34} bonds are clearly localized single and double bonds, respectively, while for **1b** the corresponding bond length is of intermediate value, around 1.40 Å, predictive of a delocalized structure. For **1b** (Figure 2 right), comparable bond lengths are found across the applied methods, but variations in the interallylic distances R are observed. The MP4 and CCSD(T) angle <456 optimized geometries (as described earlier) have interallylic distances of R = 2.11 Å and R = 2.12 Å, respectively. These methods are expected to give the best results, and therefore the other methods are compared to these. The B3LYP method, with cc-pVDZ and cc-pVTZ basis sets, gives interallylic distances similar to the highly correlated methods. So the B3LYP method appears to result in accurate geometries of **1b**, but the corresponding $\Delta H^{\ddagger}$ is too low, as discussed earlier. The MP2 method, with cc-pVDZ and cc-pVTZ basis sets, gives interallylic distances of 2.07 Å and 2.04 Å, respectively, which are shorter than the MP4 and CCSD(T) values. However, the very good results for $\Delta H^{\ddagger}$ obtained using MP4/cc-pVDZ//MP2/cc-pVDZ, made MP2/cc-pVDZ the method chosen for geometry optimizations, with the notion that the method could underestimate the interallylic distance.

The aromaticity of the investigated molecules is addressed using NICS, which is defined as the negative of the absolute magnetic shielding[36] and is a simple and efficient measure of aromaticity. A negative

NICS, like -9.7 at the ring center of benzene,[36] indicates an aromatic structure, while a positive value, like 27.6 in cyclobutadiene,[36] indicates an antiaromatic structure. A negligible value, like -2.2 in cyclohexane,[36] indicates a non-aromatic structure.

The NICS(0) of **1** is calculated at the geometric center (nonweighted mean of heavy atom coordinates) of the 6 active atoms (i.e. atoms 2,3,4,6,7 and 8, see Scheme 1). However, as discussed by Jiao,[23] this geometric center is only around 1.1 Å from the cyclopropane ring, hence the special shielding effect encountered for cyclopropane **16** needs to be taken into account when NICS is used to address aromaticity in **1**. The part of the NICS(0) at the geometric center of **1** which arises from the cyclopropane ring 1.1 Å away, is taken into account by calculating NICS 1.1 Å above the face of **16**. In Table 2 the calculated GIAO-HF/cc-pVDZ NICS values are listed. The NICS(1.1) value of -7.5 (entry 1 rigth) for **16**, is close to the –10.8 NICS(0) calculated for **1a** (entry 1 left). Hence, the cyclopropane unit is largely responsible for the calculated NICS(0) of **1a**. The calculated NICS(0) of the delocalized **1b** structure is between –22.1 and –22.9 (entry 2-4 left), which is not due to the cyclopropane unit alone, but must have a significant contribution from homoconjugation. The calculated NICS(0) of **1b** clearly shows that it is a bishomoaromatic structure. The NICS values for **1** reported herein calculated using GIAO-HF/cc-pVDZ//MP2/cc-pVDZ are in good accordance with the values reported by Jiao[23] obtained using GIAO-HF/6-31G*//Becke3LYP/6-31G*.

Similarly, the magnetic properties of the corresponding three membered rings found in **2** - **15**, namely aziridine **17**, phosphirane **18**, diaziridine **19**, and diphosphirane **20**, are relevant parameters to address when using NICS(0) to discuss the aromaticity in **2** – **15**. The calculated NICS values are given in Table 2. For **17** a NICS(1.1) value of –4.2 is calculated for the planar C_{2v} symmetric structure, while –6.1 to –6.2 is calculated at each side of the non-planar C_s symmetric structure. Similar for **18**, a NICS(1.1) value of -2.8 is calculated for the planar C_{2v} symmetric structure, and NICS(1.1) at each side of the nonplanar C_s symmetric structure is –8.1 to –9.1.

For both **17** and **18** the nonplanar structures are the most stable ones, and NICS(1.1) at the two possible 1.1 Å points (above and below the ring centers) are close and hence considered identical for all practical purposes. For **19** and **20**, one planar, one cis and one trans structure can be envisaged. The planar and the trans structures will each have a single point 1.1 Å above the ring centers, while the cis structures each will have two different points (above and below) 1.1 Å from the ring centers. The trans structures are found to be the most stable ones, closely followed by the cis structures and then the planar ones. Almost identical NICS values are calculated for the cis and trans structures of **19** (entry 4) and **20** (entry 5), while their planar structures have negligible NICS values.

Aza- and phosphasemibullvalenes

The calculated MP4 and CCSD(T) values of $\Delta H^{\ddagger}$ for **2** – **15** are presented in Table 3, while the calculated NICS(0), interallylic distances R and selected bond lengths are given in Table 4.

From geometry optimizations at the MP2/cc-pVDZ level, the delocalized, symmetric **b** structures of **5**, **7**, **9**, **11**, **12**, **13** and **15** were found to be ground state structures. Vibrational frequency calculations gave only positive frequencies, confirming that they are energy minima. Full re-optimization of these delocalized **5b**, **7b**, **9b**, **11b**, **12b**, **13b** and **15b** geometries, but now removing all symmetry constraints, in all cases gave structures that were indistinguishable from the originally optimized symmetry constrained structures. Energy minima for the localized azasemibullvalene **12a**, the phosphasemibullvalenes **5a**, **7a**, **9a**, **11a**, **13a** and **15a** could not be located at the MP2/cc-pVDZ level. Using the symmetry constrains shown in Scheme 1, these localized, low-symmetry **a** structures all optimize to structures that are indistinguishable from their corresponding higher symmetry **b** structures. Calculated MP4 and CCSD(T) energies, as well as MP2 zero-point energies, were identical for the **a** and **b** structures of **5**, **7**, **9**, **11**, **12**, **13** and **15** (Table 3). From this it follows that these molecules are

predicted not to undergo a Cope rearrangement, but have single well potentials with highly symmetric ground states. Hence, the only energy minimum that could be located at the MP2/cc-pVDZ surface for the hetero semibullvalenes **5**, **7**, **9**, **11**, **12**, **13** and **15** are the delocalized **b** structures.
At the computational levels applied herein, the early finding by Dewar[8] that **12** should be a localized structure is hence not corroborated.
The calculated C-C bond lengths (Table 4) r_{34} and r_{78} for **5**, and r_{67} and r_{78} for **7** and **9**, are between 1.40 and 1.41 Å, which is intermediate of classical single and double bond lengths. Similarly, the C-P distances r_{23} and r_{67} for **5** of 1.75 Å, and r_{23} and r_{34} for **7** of 1.74 Å, are all shorter than the C-P single bond r_{23} and longer than the C-P double bond r_{34} observed in the bond localized **3a**. For **11**, **13** and **15** all C-P bond lengths are found to be between 1.74 to 1.76 Å, which is of intermediate length like in bond delocalized **3b**. For **12**, a C-N bond length of 1.35 Å is calculated, which is in between the C-N single and double bonds found for **2a**. These geometric findings all points at delocalized bonds in **5**, **7**, **9**, **11**, **12**, **13** and **15**.
The calculated NICS(0) values of the delocalized ground states **5**, **7**, **9**, **11**, **12**, **13** and **15** are all large and negative (Table 4). They span from -19.3 for **15** to -22.8 for **7**. The values are comparable to NICS(0) calculated for delocalized semibullvalene **1b** (Table 2). When the calculated NICS(1.1) value of **18,** up to –9.1 (Table 2), is taken into account when considering the values calculated for **5**, **7**, **9**, **11** and **15**, evidently there remains major contributions attributably only to these molecules being homoaromatic. Similarly, considering the calculated NICS(1.1) of **19** and **20** (Table 2) clearly leaves **12** and **13**, respectively, homoaromatic based on their calculated NICS(0) values.
The NICS method has previously been applied to a tetraphosphabarbaralane related to **13**, although in a more advanced molecular dynamics framework,[35] where the homoaromatic nature was confirmed when addressing temporal evolution and temperature dependency.

The interallylic distances R in **5**, **7**, **9**, **11** and **15** are between 2.20 and 2.28 Å. They are C-P bonds and are hence expected to be somewhat longer than R in **1b**. For **13**, the interallylic P-P bond length is calculated to be 2.49 Å, which is in good agreement with the time dependent average of 2.53 Å calculated for the related tetraphosphabarbaralane.[35] For **12** the N-N interallylic R is 2.10 Å, comparable to R in **1b**. These short N-N and P-P interallylic distances indicate good through-space interactions between the two allylic fragments. However, Brown et al.[13] discussed that substituted semibullvalenes with C_{2v} geometries not necessarily benefit from bishomoaromatic stabilization. This was observed in derivatives of **1** having large interallylic distances (>2.5Å), reduced interallylic through-space interaction and wavefunctions with large amount of diradical character or even triplet groundstates. To address this issue, the geometries of **5**, **7**, **9**, **11**, **12**, **13** and **15** where optimized at the UHF-MP2/cc-pVDZ level. All wavefunctions were found to be pure singlets with $\langle S^2 \rangle$=0.00, and the UHF-MP2 geometries were indistinguishable from the RHF-MP2 geometries. This further corroborates that **5**, **7**, **9**, **11**, **12**, **13** and **15** are delocalized and bishomoaromatic.
For the azasemibullvalenes **2**, **4**, **6**, **8**, **10** and **14**, and the phosphasemibullvalene **3** energy minima for both the localized **a** and delocalized **b** structures could be identified at the MP2/cc-pVDZ surface. Vibrational frequency analyses showed that all localized **a** structures had positive frequencies only, while delocalized **b** structures had 1 imaginary frequency, except for **4**, **8** and **14**. The latter **b** structures had all positive vibrational frequencies, indicating that these structures could also be energy minima.
The calculated activation enthalpy for **2** is comparable to semibullvalene, while it is somewhat higher for **3**. For **4**, **6**, **8**, **10** and **14** the calculated activation enthalpies are several kcal/mol lower than semibullvalene. Notably **4** and **6** have very low calculated barriers to the Cope rearrangement, below 1 kcal/mol at MP4 and around 3 kcal/mol at CCSD(T). For **4** and **6**, and possibly also **8**, **10** and **14**, the calculated $\Delta H^{\ddagger}$ values are so small that these molecules in reality could be delocalized ground states structures.

At the computational levels applied herein, the early finding by Dewar[25] that 3,7-diazasemibullvalene **2** should be 'nonclassical' is hence not corroborated. Both **2** and the phospha derivative **3** have clear barriers to the Cope rearrangement.

The localized ground states **2a**, **3a**, **4a**, **6a**, **8a**, **10a** and **14a** all have calculated NICS(0) values that are negative but clearly smaller than the corresponding delocalized **b** structures (Table 4). When NICS(1.1) of **16** is taken into account for **2a** and **3a**, their remaining NICS are -5.4 and 1.3, respectively, clearly suggesting non-aromatic ground state structures. Similarly, when NICS(1.1) of **17** is accounted for, the remaining NICS(0) for **6a** and **10a** is -4.9 and -4.8, respectively, pointing at non-aromatic structures. However, for **4a**, **8a** and **14a** NICS(0) values after accounting for NICS(1.1) of **17**, are -10.4, -7.6 and -9.4, respectively, suggesting aromatic structures. As discussed earlier **4**, **8** and **14** have very low $\Delta H^{\ddagger}$ values, which together with their large negative NICS(0) suggests that they could be more delocalized than localized. This is in line with Dewar's[8,25] finding that **4** should actually be 'nonclassical'.

The calculated $\Delta H^{\ddagger}$ for **4** is clearly lower than $\Delta H^{\ddagger}$ calculated for **1**. This trend is supported by the experimental observations[26-28] on a 3,7-diphenyl derivative as well as on a 4,8-dicyano-3,7-diphenyl derivative of **4**. In both cases, a drastic increase in the rate to the Cope rearrangement was observed. The actual nature of the ground state of molecules based on structures like **4**, **8** and **14**, that is to which extend homoconjugation is present, is highly influenced by parameters like additional substituents, solvent and temperature[44,45].

Conclusions

Using correlated *ab initio* methods the tetraazasemibullvalene **12**, the phosphasemibullvalenes **5**, **7**, **9**, **11**, **13** and **15** were shown to have highly symmetric, delocalized minima, possessing large, negative NICS values, which together with calculated bond lengths suggests that these molecules are highly bishomoaromatic. Furthermore, **4**, **8** and **14** could also be bishomoaromatic structures due to their calculated NICS(0) values and very low $\Delta H^{\ddagger}$. Appropriate introduction of two, three and four N or P atoms in the semibullvalene sceleton appears as a succesfull design strategy towards homoaromatic semibullvalene structures.

Supplementary material

Calculated energies and coordinates are available online as supplementary material.

References

1. A.K. Cheng, F.A.L. Anet, J. Mioduski, J. Meinwald, *J. Am. Chem. Soc.* **1974**, *96*, 2887-2891.
2. D. Moskau, R. Aydin, W. Leber, H. Günther, H. Quast, H.D. Martin, K. Hassenrück, L.S. Miller, K. Grohmann, *Chem. Ber.* **1989**, *122*, 925-931.
3. R.V. Williams, *Chem. Rev.* **2001**, *101*, 1185-1204.
4. R.V. Williams, *Eur. J. Org. Chem.* **2001**, 227-235.
5. M. J. S. Dewar, D.H Lo, *J. Am. Chem. Soc.* **1971**, *93*, 7201-7207.
6. R. Hoffmann, W.D. Stohrer, *J. Am. Chem. Soc.* **1971**, *93*, 6941-6948.
7. L.S. Miller, K. Grohmann, J.J. Dannenberg, *J. Am. Chem. Soc.* **1983**, *105*, 6862-6865.
8. M.J.S. Dewar, C. Jie, *Tetrahedron* **1988**, *44*, 1351-1358.
9. H. Quast, R. Janiak, E.M. Peters, K. Peters, H.G.v. Schnering, *Chem. Ber.* **1992**, *125*, 969-973.
10. L.M. Jackman, E. Fernandes, M. Heubes, H. Quast, *Eur. J. Org. Chem.* **1998**, 2209-2227.
11. D.A. Hrovat, R. V. Williams, A. C. Goren, W. T. Borden, *J. Comp. Chem.* **2001**, *22*, 1565-1573.
12. A.C. Goren, D. A. Hrovat, M. Seefelder, H. Quast, W.T. Borden, *J. Am. Chem. Soc.* **2002**, *124*, 3469-3472.
13. E.C. Brown, D.K. Henze, W.T. Borden, *J. Am. Chem. Soc.* **2002**, *124*, 14977-14982.
14. H.S. Wu, H. Jiao, Z.X. Wang, P.v.R. Schleyer, *J. Am. Chem. Soc.* **2003**, *125*, 10524-10525.
15. H.S. Wu, J. Jia, H. Jiao, *J. Mol. Model.* **2007**, *13*, 133-136.
16. H. Jiao, P.v.R. Scleyer, *Angew. Chem. Int. Ed. Engl.* **1993**, *32*, 1760-1763.
17. S.C. Wang, D.J. Tantillo, *J. Phys. Chem. A* **2007**, *111*, 7149-7153.
18. E. Vogel, U.H. Brinker, K. Nachtkamp, J. Wassen, K. Müllen, *Ang. Chem. Int. Ed. Engl.* **1973**, *12*, 758-761.
19. R.V. Williams, H.A. Kurtz, B. Farley, *Tetrahedron* **1988**, *44*, 7455-7460.
20. R.V. Williams, H.A. Kurtz, *J. Org. Chem.* **1988**, *53*, 3626-3628.
21. R.V. Williams, H.A. Kurtz, *J. Chem. Soc. Perkin Trans. 2* **1994**, 147-150.
22. R.V. Williams, V.R. Gadgil, K. Chauhan, *J. Am. Chem. Soc.* **1996**, *118*, 4208-4209.

23. H. Jiao, R. Nagelkerke, H.A. Kurtz, R. V. Williams, W.T. Borden, P.v.R Schleyer, *J. Am. Chem. Soc.* **1997**, *119*, 5921-5929.

24. R.V. Williams, V.R. Gadgil, K. Chauhan, *J. Org. Chem.* **1998**, *63*, 3302-3309.

25. M.J.S. Dewar, Z. Náhlovská, B.D. Náhlovský, *Chem. Com.* **1971**, *21*, 1377-1378.

26. C. Schnieders, H.J. Altenbach, K. Müllen, *Ang. Chem. Int. Ed. Engl.* **1982**, *21*, 637-638.

27. C. Schnieders, W. Huber, J. Lex, K. Müllen, *Ang. Chem. Int. Ed. Engl.* **1985**, *24*, 576-577.

28. B. Düll, K. Müllen, *Tet. Let.* **1992**, *33*, 8047-8050.

29. R. Gompper, M. Schwarzensteiner, *Ang. Chem. Int. Ed. Engl.* **1983**, *22*, 543-544.

30. J. Geier, G. Frison, H. Grützmacher, *Ang. Chem. Int. Ed. Engl.* **2003**, *42*, 3955-3957.

31. P. Binger, S. Stutzmann, J. Bruckmann, C. Krüger, J. Grobe, D.L. Van, T. Pohlmeyer, *Eur. J. Inorg. Chem.* **1998**, 2071-2074.

32. A. Mack, B. Breit, T. Wettling, U. Bergsträsser, S. Leininger, M. Regitz, *Ang. Chem. Int. Ed. Engl.* **1997**, *36*, 1337-1340.

33. D. Moskau, W. Leber, H. Günther, R. Gompper, P. Spes, *Chem. Ber.* **1989**, *122*, 2361-2364.

34. M. Reiher, B. Kirchner, *Ang. Chem. Int. Ed. Engl.* **2002**, *41*, 3429-3433.

35. B. Kirchner, D. Sebastiani, *J. Phys. Chem. A* **2004**, *108*, 11728-11732.

36. P.v.R Schleyer, C. Maerker, A. Dransfeld, H. Jiao, N.J.R.v.E. Hommes, *J. Am. Chem. Soc.* **1996**, *118*, 6317-6318.

37. T.H. Dunning Jr., *J. Chem. Phys.* **1989**, *90*, 1007-1023.

38. M.W. Schmidt, K.K. Baldridge, J.A. Boatz, S.T. Elbert, M.S. Gordon, J.H. Jensen, S. Koseki, N. Matsunaga, K.A. Nguyen, S.Su, T.L.Windus, M.Dupuis, J.A.Montgomery Jr., *J. Comp. Chem.* **1993**, *14*, 1347-1363.

39. A.A. Granovsky, *PC Gamess* **2004**.

40. N. Bandeira, E. Schumacher, *WinGamess* **2004**.

41. Basis sets were obtained from the Extensible Computational Chemistry Environment Basis Set Database, Version 7/30/02, as developed and distributed by the Molecular Science Computing Facility, Environmental and Molecular Sciences Laboratory which is part of the Pacific Northwest Laboratory, P.O.Box 999, Richland, Washington 99352, USA, and funded by the U.S.Department of Energy.The Pacific Northwest Laboratory is a multi-program laboratory operated by Battelle Memorial Institue for the U.S.Department of Energy under contract DE-AC06-76RLO 1830.Contact David Feller or Karen Schuchardt for further information.

42. E. J. Bylaska, W. A. de Jong, N. Govind, K. Kowalski, T. P. Straatsma, M. Valiev, D. Wang, E. Apra, T. L. Windus, J. Hammond, P. Nichols, S. Hirata, M. T. Hackler, Y. Zhao, P.-D. Fan, R. J. Harrison, M. Dupuis, D. M. A. Smith, J. Nieplocha, V. Tipparaju, M. Krishnan, Q. Wu, T. Van Voorhis, A. A. Auer, M. Nooijen, E. Brown, G. Cisneros, G. I. Fann, H. Fruchtl, J. Garza, K. Hirao, R. Kendall, J. A. Nichols, K. Tsemekhman, K. Wolinski, J. Anchell, D. Bernholdt, P. Borowski, T. Clark, D. Clerc, H. Dachsel, M. Deegan, K. Dyall, D. Elwood, E. Glendening, M. Gutowski, A. Hess, J. Jaffe, B. Johnson, J. Ju, R. Kobayashi, R. Kutteh, Z. Lin, R. Littlefield, X. Long, B. Meng, T. Nakajima, S. Niu, L. Pollack, M. Rosing, G. Sandrone, M. Stave, H. Taylor, G. Thomas, J. van Lenthe, A. Wong, and Z. Zhang, "NWChem, A Computational Chemistry Package for Parallel Computers, Version 5.1" (2007), Pacific Northwest National Laboratory, Richland, Washington 99352-0999, USA.

R.A. Kendall, E. Apra, D.E. Bernholdt, E.J. Bylaska, M. Dupuis, G.I. Fann, R.J. Harrison, J. Ju, J.A. Nichols, J. Nieplocha, T.P. Straatsma, T.L. Windus, A.T. Wong, *Comp. Phys. Comm.* **2000**,*128*, 260-283.

43. F. Jensen, *Introduction to Computational Chemistry*, John Wiley & Sons Ltd., **1999**.

44. M. Seefelder, H. Quast, *Ang. Chem. Int. Ed. Engl.* **1999**, *38*, 1068-1071.

45. M. Seefelder, M. Heubes, H. Quast, W.D. Edwards, J. R. Armantrout, R.V. Williams, C.J. Cramer, A.C. Goren, D.A. Hrovat, W.T. Borden, *J. Org. Chem.* **2005**, *70*, 3437-3449.

46. Y.C. Wang, S.H. Bauer, *J. Am. Chem. Soc.* **1972**, *94*, 5651-5657.

Table 1. Calculated activation enthalpies $\Delta H^{\ddagger}$ (kcal/mol)[a] of **1** at different levels of theory.

	Level	$\Delta H^{\ddagger}$		Level	$\Delta H^{\ddagger}$		Level	$\Delta H^{\ddagger}$
1	HF/cc-pVDZ[b]	15.70	7	MP2/cc-pVTZ[e]	0.94	13	(6,6)CASSCF/cc-pVDZ[h]	23.54
2	MP2/cc-pVDZ[c]	2.25	8	MP3/cc-pVTZ[e]	9.76	14	CCSD/cc-pVDZ[c]	10.61
3	MP3/cc-pVDZ[c]	10.80	9	MP4/cc-pVTZ[e]	3.67	15	CCSD(T)/cc-pVDZ[c]	7.31
4	MP4/cc-pVDZ[c]	5.10	10	"MP-∞"/cc-pVTZ	4.73	16	CCSD(T)/cc-pVDZ[i]	7.10
5	MP4/cc-pVDZ[d]	4.91	11	Becke3LYP/cc-pVDZ[f]	4.30	17	Experiment[1,2]	4.8-5.2
6	"MP-∞"/cc-pVDZ	4.95	12	Becke3LYP/cc-pVTZ[g]	3.80			

[a]$\Delta H^{\ddagger}$ = ΔE + ΔZPE, where ΔE is the energy difference between the C_{2v} (**1b**) and C_s (**1a**) semibullvalene, and ΔZPE = -0.95 kcal/mol is the corresponding difference in zero-point vibrational energies taken from MP2/cc-pVDZ calculations. [b]HF/cc-pVDZ optimized geometries. [c]MP2/cc-pVDZ optimized geometries. [d] MP4/cc-pVDZ optimized <456 geometries, see text. [e]MP2/cc-pVTZ optimized geometries. [f]Becke3LYP/cc-pVDZ optimized geometries. [g] Becke3LYP/cc-pVTZ optimized geometries. [h] (6,6)CASSCF/cc-pVDZ optimized geometries. [i] CCSD(T)/cc-pVDZ optimized <456 geometries, see text.

Table 2. Calculated GIAO-HF/cc-pVDZ NICS(0) (ppm) for **1a**, **1b** and NICS(1.1) (ppm) for **16** - **20**.

Molecule	NICS(0)[a]	Molecule	NICS(1.1)[b]
1a[c]	-10.8	**16**[c]	-7.5
1b[c]	-22.9	**17**[c]	-4.2[f], -6.1[g], -6.2[g]
1b[d]	-22.4	**18**[c]	-2.8[f], -8.1[g], -9.1[g]
1b[e]	-22.1	**19**[c]	-0.6[f], -4.7[h], -5.6[h], -5.3[i]
		20[c]	-0.3[f], -8.8[h], -9.2[h], -9.9[i]

[a]NICS calculated at ring center. [b]NICS calculated 1.1 Å above ring center.
[c]MP2/cc-pVDZ optimized geometries.
[d]MP4/cc-pVDZ optimized angle geometries, see text.
[e]CCSD(T)/cc-pVDZ optimized angle geometries, see text.
[f]NICS(1.1) of planar structure. [g]NICS(1.1) of non-planar structure.
[h]NICS(1.1) of cis structure. [i]NICS(1.1) of trans structure.

Table 3. Calculated MP4 and CCSD(T) energy differences, ΔE^{MP4} and ΔE^{CC} respectively (kcal/mol), MP2 Zero-Point Energy differences ΔZPE^{MP2} (kcal/mol) and MP4 and CCSD(T) activation enthalpies, $\Delta H^{\ddagger MP4}$ and $\Delta H^{\ddagger CC}$ respectively (kcal/mol).[a]

Molecule	ΔE^{MP4}	$\Delta H^{\ddagger MP4}$	ΔE^{CC}	$\Delta H^{\ddagger CC}$	ΔZPE^{MP2}	Molecule	ΔE^{MP4}	$\Delta H^{\ddagger MP4}$	ΔE^{CC}	$\Delta H^{\ddagger CC}$	ΔZPE^{MP2}
2	6.35	5.40	8.55	7.60	-0.95	**9**[b]	0.00	0.00	0.00	0.00	0.00
3	10.94	9.84	13.94	12.84	-1.10	**10**	2.72	2.02	4.36	3.66	-0.70
4	0.79	0.56	3.34	3.11	-0.23	**11**[b]	0.00	0.00	0.00	0.00	0.00
5[b]	0.00	0.00	0.00	0.00	0.00	**12**[b]	0.00	0.00	0.00	0.00	0.00
6	1.39	0.83	3.27	2.71	-0.56	**13**[b]	0.00	0.00	0.00	0.00	0.00
7[b]	0.00	0.00	0.00	0.00	0.00	**14**	2.06	2.03	4.71	4.68	-0.03
8	1.83	1.68	4.25	4.10	-0.15	**15**[b]	0.00	0.00	0.00	0.00	0.00

[a] $\Delta H^{\ddagger} = \Delta E + \Delta ZPE$, where ΔE is the energy difference between the more symmetric **b** and less symmetric **a** structures and ΔZPE is the corresponding difference in zero-point vibrational energies taken from MP2/cc-pVDZ calculations. [b] For these structures no localized energy minimum could be located. The **a** structures, optimized without any symmetry constraints, are indistinguishable from the symmetry constrained **b** structures.

Table 4. Calculated Nucleus Independent Chemical Shifts NICS(0) (ppm), interallylic distances R[a] (Å), bond lengths r_{23}, r_{34}, r_{67} and r_{78} (Å).

Molecule	NICS(0)	R	r_{23}	r_{34}	r_{67}	r_{78}	Molecule	NICS(0)	R	r_{23}	r_{34}	r_{67}	r_{78}
2a	-12.9	2.25	1.42	1.30	1.30	1.42	**9a**[b]	-21.4	2.25	2.12	2.12	1.41	1.41
2b	-24.9	1.95	1.35	1.35	1.35	1.35	**9b**[b]	-21.4	2.25	2.12	2.12	1.41	1.41
3a	-6.2	2.36	1.85	1.71	1.71	1.85	**10a**	-11.0	2.25	1.41	1.30	1.30	1.42
3b	-18.8	1.98	1.76	1.76	1.76	1.76	**10b**	-20.4	2.00	1.35	1.35	1.34	1.34
4a	-16.6	2.27	1.42	1.36	1.31	1.46	**11a**[b]	-20.8	2.23	1.74	1.74	1.76	1.76
4b	-23.3	2.08	1.35	1.40	1.35	1.40	**11b**[b]	-20.8	2.23	1.74	1.74	1.76	1.76
5a[b]	-22.4	2.28	1.75	1.40	1.75	1.40	**12a**[b]	-22.1	2.10	1.35	1.35	1.35	1.35
5b[b]	-22.4	2.28	1.75	1.40	1.75	1.40	**12b**[b]	-22.1	2.10	1.35	1.35	1.35	1.35
6a	-11.1	2.28	1.41	1.30	1.37	1.47	**13a**[b]	-21.7	2.49	1.75	1.75	1.75	1.75
6b	-17.8	2.05	1.35	1.35	1.40	1.40	**13b**[b]	-21.7	2.49	1.75	1.75	1.75	1.75
7a[b]	-22.8	2.26	1.74	1.74	1.40	1.40	**14a**	-15.6	2.19	1.41	1.31	1.28	1.41
7b[b]	-22.8	2.26	1.74	1.74	1.40	1.40	**14b**	-27.3	1.98	1.33	1.34	1.33	1.34
8a[b]	-13.8	2.24	1.41	1.27	1.37	1.46	**15a**[b]	-19.3	2.20	2.14	1.76	2.14	1.76
8b[b]	-23.8	2.01	1.33	1.33	1.40	1.40	**15b**[b]	-19.3	2.20	2.14	1.76	2.14	1.76

[a] For localized structures R is taken as r_{46}. [b] For these structures no localized energy minimum could be located. The **a** structures, optimized without any symmetry constraints, are indistinguishable from the symmetry constrained **b** structures.